ISSN 0023-1584, Kinetics and Catalysis, 2008, Vol. 49, No. 4, pp. 466–473. © MAIK "Nauka/Interperiodica" (Russia), 2008.
Original Russian Text © G.A. Skorobogatov, V.K. Khripun, A.G. Rebrova, 2008, published in Kinetika i Kataliz, 2008, Vol. 49, No. 4, pp. 489–496.

Isochoric Isothermal Pyrolysis of Trifluoroiodomethane: $CF_3^{\bullet}$ Recombination Kinetics

G. A. Skorobogatov, V. K. Khripun, and A. G. Rebrova

Faculty of Chemistry, St. Petersburg State University, St. Petersburg, 198504 Russia

e-mail: skorgera@mail.ru

Received November 14, 2007

Abstract—The rate constant of $CF_3^{\bullet}$ recombination ($k^{M}_{(CF_3)_2}$) in the isochoric isothermal pyrolysis of trifluoroiodomethane at $T = 625$–732 K and $P = 29$–300 Torr was derived from molecular iodine accumulation curves. Using literature data for the high-pressure limit and the results of our measurements, an analytical expression for $k^{M}_{(CF_3)_2}$ was set up for $T = 300$–1300 K and any pressure of the buffer gas CF_3I.

DOI: 10.1134/S0023158408040022

The isochoric isothermal pyrolysis (IIP) method was used earlier in the kinetic study of thermal gas-phase reactions of perfluoroalkyl iodides (CF_3I, C_2F_5I, C_3F_7I, etc.) and trifluorobromomethane (CF_3Br) [1–4]. The perfluoroalkyl halide RX subjected to IIP decomposes at a fixed temperature under mild conditions. The overall process is limited to the reaction

$$RX \longrightarrow 1/2R_2 + 1/2X_2. \quad \text{(I)}$$

The detailed mechanism of the overall reaction (I) is described by scheme (II)–(V), which does not include any cleavage or polymerization reactions of the radical $R^{\bullet}$:

$$RX \longleftrightarrow R^{\bullet} + X^{\bullet}, \quad K_{c,2} = k_2/k_{-2} = [R]_{eq}[X]_{eq}/[RX]_{eq}, \quad \text{(II)}$$

$$X^{\bullet} + RX \longleftrightarrow R^{\bullet} + X_2, \quad K_{c,3} = k_3/k_{-3} = K_{c,2}/K_{c,4}, \quad \text{(III)}$$

$$2X^{\bullet} + M \longleftrightarrow X_2 + M, \quad K_{c,4} = k_4/k_{-4} = [X]^2_{eq}/[X_2]_{eq}, \quad \text{(IV)}$$

$$2R^{\bullet} + M \longrightarrow R_2 + M, \quad k_5 = -1/2(d[R]/dt)[R]^{-2}. \quad \text{(V)}$$

Here, M is a third particle (M = RX, R_2, X_2, $R^{\bullet}$, $X^{\bullet}$, or an inert diluent gas (Ar, He, etc.)); $[R]_{eq}$, $[X]_{eq}$, and $[RX]_{eq}$ are the equilibrium concentrations of R, X, and RX; $k_i(k_{-i})$ is the rate constant of the ith forward (reverse) reaction; and $K_{c,i}$ is the constant of the ith equilibrium.

The rate of the overall process is limited by the rate of reaction (V) (which is irreversible under the IIP conditions). It is, therefore, possible to derive the rate constant k_5 from the accumulation rate of the recombination product R_2 or, more conveniently, from the accumulation rate of the molecular halogen X_2. In our previous studies [1–4], our primary concern was to conduct reaction (I) at a total gas pressure sufficiently high for the recombination reaction (V) to obey a second-order rate law (in the high-concentration limit). The IIP method can be adapted for k_5 measurements in the intermediate pressure range and even down to the low pressures at which the recombination reaction (V) is third-order. Here, we report recombination rate constant measurements for trifluoroiodomethane, CF_3I.

COMPUTATIONAL ALGORITHM

In this work, as distinct from our previous studies [1–4], we will take into account that reaction (V) involving polyatomic radicals proceeds via the ET mechanism [5]:

$$2R^{\bullet} \underset{k_{-a}}{\overset{k_a}{\rightleftarrows}} R_2^{\neq}, \quad R_2^{\neq} + M_i \xrightarrow{k_i^*} R_2 + M_i. \quad \text{(VI)}$$

Accordingly, the apparent second-order recombination rate constant k_5 depends both on the reaction temperature (T) and on the total pressure of the reaction mixture (P):

$$k_5(T, P) = k_{R_2} = \frac{k_a}{1 + \left(k_{-a}/\sum_i k_i^*[M_i] \right)}. \quad (1)$$

We will take into account that the $R^{\bullet}$ radicals can disappear both via recombination and via diffusion to the reactor wall, where they ultimately form the same dimer R_2. This dimer is desorbed from the wall and returns into the reaction space:

$$R^{\bullet} \xrightarrow{k_D} R^{\bullet}\ (\text{on the wall}) \longrightarrow 1/2R_2\uparrow, \quad k_D = -(d[R]/dt)[R]^{-1}. \quad \text{(V')}$$

The diffusion loss rate constant ($k_{D,P}$) depends on the total gas pressure:

$$k_{D,P} = k_D^* \frac{\sqrt{T/300\ \mathrm{K}}}{(P/760\ \mathrm{Torr})}, \quad (2)$$

$$k_D^* = \left(\frac{\pi^2}{l^2} + \frac{5.78}{r^2}\right) D_R^*, \quad (3)$$

where l is the length of the cylindrical reactor; r is the radius of the reactor; and k_D^* and D_R^* are, respectively, the diffusion rate constant (s^{-1}) and the diffusion coefficient (cm^2/s) of the radical R• at 300 K and a buffer gas pressure of 760 Torr.

Following Kondrat'ev [6], we will assume that, in Eq. (1), k_a and k_i^* depend on temperature like the number of gas-kinetic collisions and k_{-a} obeys the Arrhenius law:

$$\begin{aligned} k_a &= k_{R_2}(300\ \mathrm{K})\sqrt{T/300\ \mathrm{K}}, \\ k_i^* &= k_i^*(300\ \mathrm{K})\sqrt{T/300\ \mathrm{K}}, \\ k_{-a} &= a\exp\left(-\frac{b}{T}\right). \end{aligned} \quad (4)$$

Substituting Eq. (4) into Eq. (1) yields

$$\begin{aligned} k_{R_2} &= \frac{k_a}{1 + \left(k_{-a}/\sum_i k_i^*[M_i]\right)} \\ &= \frac{\sqrt{T/300\ \mathrm{K}}\,k_{R_2}(300\ \mathrm{K})}{1 + \left(\dfrac{a}{[RX]_0\sqrt{T/300\ \mathrm{K}}\sum \mu_i k_i^*(300\ \mathrm{K})}\right)e^{-\frac{b}{T}}}, \end{aligned} \quad (5)$$

where $\mu_i = [M_i]/[RX]_0$ is the mole fraction of the ith component with respect to the initial halide RX. IIP experiments are conducted so that the amount of decomposed halide does not exceed a few hundredths of the initial amount of RX. If this is the case, all μ_i values but $\mu_{RX} \approx 1$ under the summation sign in Eq. (5) can be neglected to obtain

$$k_{R_2} = \frac{\sqrt{T/300\ \mathrm{K}}\,k_{R_2}(300\ \mathrm{K})}{1 + \left(\dfrac{a}{[RX]_0\sqrt{T/300\ \mathrm{K}}\,k_{RX}^*(300\ \mathrm{K})}\right)e^{-\frac{b}{T}}}. \quad (6)$$

Such a kinetic experiment on pyrolysis (reaction (I)) enables one to determine the following four unknown quantities: $k_{R_2}(300\ \mathrm{K})$, $a/k_{RX}^*(300\ \mathrm{K})$, b, and $D_{R,RX}^*$ (diffusion coefficient of the radical R• in the gas RX under normal conditions).

The experiment can also be conducted in another way: the halide RX can be diluted with a large amount of the buffer gas M. In this case, all μ_i values but $\mu_M = [M]/[RX]_0$ under the summation sign in Eq. (5) can be neglected at any extent of decomposition of the halide:

$$k_{R_2} = \frac{\sqrt{T/300\ \mathrm{K}}\,k_{R_2}(300\ \mathrm{K})}{1 + \left(\dfrac{a}{[M]\sqrt{T/300\ \mathrm{K}}\,k_M^*(300\ \mathrm{K})}\right)e^{-\frac{b}{T}}}. \quad (6')$$

The following four quantities can be derived from this kinetic experiment: $k_{R_2}(300\ \mathrm{K})$, $(a/k_M^*(300\ \mathrm{K}))$, b, and $D_{R,M}^*$ (diffusion coefficient of the radical R• in the gas M under normal conditions).

The following kinetic equations correspond to reactions (II)–(V) and (V'):

$$\begin{aligned} \frac{d[R]}{dt} &= k_2[RX] - k_{-2}[R][X] + k_3[X][RX] \\ &\quad - k_{-3}[R][X_2] - 2k_5(P,T)[R]^2 - k_{D,P}[R], \\ \frac{d[X]}{dt} &= k_2[RX] - k_{-2}[R][X] \\ &\quad - 2k_4[M][X]^2 + 2k_{-4}[M][X_2], \\ \frac{d[R_2]}{dt} &= k_5(P,T)[R]^2 + k_{D,P}[R]. \end{aligned} \quad (7)$$

The set of three equations (7) is sufficient for unambiguously solving of the kinetic problem since the concentrations of the other components can be determined with a high degree of accuracy using the following balance equations:

$$[RX]_t = [RX]_0 - 2[X_2]_t, \quad [X_2]_t = [R_2]_t. \quad (8)$$

The concentrations of the reactive intermediates rapidly become constant at the given temperature, almost reaching their equilibrium values, which change slowly as the initial halide RX is consumed. This makes it possible to use the Bodenstein–Semenov quasi-steady-state approximation [7]. From the first two equations of system (7), skipping the operation of integration, we thus obtain

$$[X]_t = \sqrt{K_{c,4}[X_2]_t}, \quad (9)$$

$$[R]_t = K_{c,2}([RX]_0 - 2[X_2]_t)/(K_{c,4}[X_2])^{0.5}. \quad (10)$$

Integration of the third equation of system (7) is also unnecessary because, in the IIP experiment, the rate of increase of the molecular halogen concentration, $r(t)$, is measured directly:

$$\begin{aligned} r(t) &= \frac{d[X_2]}{dt} = \frac{d[R_2]}{dt} \\ &= k_{R_2}(P,T)[R]^2 + k_{D,P}[R]. \end{aligned} \quad (11)$$

Table 1. Pyrolysis products of alkyl halides (T = 500–800 K)

Compound	Hypothetical radical R$^{\bullet}$ ($\Delta_f H^0_{298}$, kJ/mol)	Identified recombination product (R_2)	Other identified pyrolysis products
CF_3I*	$CF_3^{\bullet}$ (–471)	C_2F_6 (100%)	I_2
C_2F_5I**	$C_2F_5^{\bullet}$ (–921)	C_4F_{10} (100%)	I_2
C_3F_7I**	$C_3F_7^{\bullet}$ (–1283)	C_6F_{14} (98%)	I_2, C_3F_6, C_3F_8
CF_3Br**	$CF_3^{\bullet}$ (–471)	C_2F_6 (100%)	Br_2
C_2H_5I**	$C_2H_5^{\bullet}$ (+125)	No	I_2, C_2H_4, C_2H_6, C_6H_6
CF_2HBr*	$CF_2H^{\bullet}$ (–243)	$C_2F_4H_2$ (2%)	Br_2, HBr, $C_3F_6H_2$, C_3F_5H, C_2F_5H, C_2F_4
CF_2ClBr*	$CF_2Cl^{\bullet}$ (–280)	$C_2F_4Cl_2$ (3%)	Br_2, HBr, C_2F_4, C_2F_4ClBr, C_3F_6ClBr, C_4F_8ClBr, C_3F_6
CH_3I*	$CH_3^{\bullet}$ (+147)	No	I_2, CH_4, C_{solid}
CH_2I_2*	$CH_2I^{\bullet}$ (+230)	No	I_2, CH_4, C_{solid}
CHI_3*	$CHI_2^{\bullet}$ (+334)	No	I_2, CH_4, C_{solid}

* This work.
** Quoted from [1–4].

By substituting Eqs. (9) and (10) into Eq. (11), we establish an analytical relationship between the sought rate constants and the measurable quantities:

$$k_{R_2}(P, T) + k_{D,P}\frac{\sqrt{K_{c,4}[X_2]}}{K_{c,2}[RX]} = \alpha(T)\frac{K_{c,4}}{K_{c,2}^2}, \qquad (12)$$

where

$$\alpha(T) = r(t)[X_2]_t/([RX]_0 - 2[X_2]_t)^2. \qquad (13)$$

Here, $[RX]_0$ is the initial halide concentration, $[X_2]_t$ is the molecular halogen concentration measured at the point in time t, and $\alpha(T)$ is the kinetic invariant independent of the current component concentrations and depending on the isothermal process temperature T.

By substituting Eqs. (2) and (6) into Eq. (12), we obtain the working formula

$$\frac{k_{R_2}(300\ \mathrm{K})K_{c,2}([RX]_0^2/2.5\times10^{19})}{\left(1+\dfrac{x\exp(-y/T)}{([RX]_0/2.5\times10^{19})\sqrt{T/300}}\right)\sqrt{K_{c,4}[X_2]}} + z = \frac{\alpha(T)([RX]_0^2/2.5\times10^{19})K_{c,4}}{\sqrt{T/300}K_{c,2}\sqrt{K_{c,4}[X_2]}} = \beta, \qquad (14)$$

where $z = k_D^*$ (s^{-1}), $y = b$, and $x = a(2.5\times10^{19}$ molecule/cm^3 $k_{RX}^*(300\ \mathrm{K}))^{-1}$ is a dimensionless quantity introduced in order to simplify the calculations.

The equilibrium constant $K_{c,4}(T)$ is known for all of the halides. Therefore, for the halogens for which $K_{c,2}(T)$ data are available, it is possible to derive the four unknowns—k_{R_2} (300 K), x, y, and z—from the values of the invariant $\alpha(T)$ measured for four combinations of T and [RX]. If kinetic measurements are made for $n > 4$ combinations of temperatures and pressures, then Eq. (14) will appear as an overdetermined system consisting of $n > 4$ algebraic equations and will be solvable by least squares. This will increase the accuracy of the calculated data.

When the diffusion loss of the radicals on the wall is negligible [8], Eq. (12) leads to the following simple expression for the second-order rate constant [1–4]:

$$k_5(T) = \alpha(T)K_{c,4}(T)/(K_{c,2}(T))^2. \qquad (15)$$

EXPERIMENTAL

For safe processing of the experimental kinetic curves using formulas (1)–(14), it is necessary to make sure that the pyrolysis reaction indeed proceeds via mechanism (II)–(V). This requires that at least the overall scheme (I) be valid. For this reason, the ultimate pyrolysis products were identified chromatographically and mass-spectrometrically for some of the simplest halides (Table 1).

For the CH_3I and CH_2I_2 gases, chromatographic and mass spectrometric analyses of the pyrolysis products demonstrated the complete absence of ethane (and diiodoethane in the case of CH_2I_2), which is the $CH_3^{\bullet}$ ($CH_2I^{\bullet}$) recombination product. Instead, only methane and molecular iodine were detected in the bulk and a carbon polymer was detected on the cell walls in both cases (Table 1). For CF_2HBr and CF_2ClBr, the pyrolysis

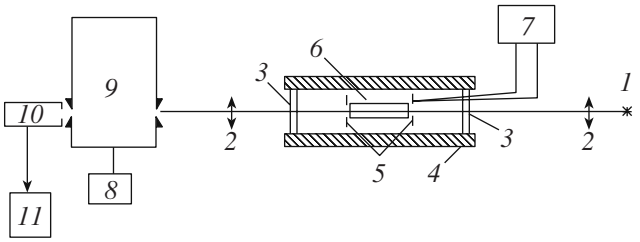

Fig. 1. Experimental setup for kinetic measurements: (*1*) DDS-30 or DVS-25 lamp, (*2*) quartz lenses, (*3*) quartz end windows, (*4*) temperature-controlled metallic heater (accuracy of ±1 K), (*5*) diaphragms, (*6*) quartz reactor (diameter, d = 30 mm; length, l = 100–150 mm), (*7*) PP-63 potentiometer, (*8*) working frequency selector of the monochromator, (*9*) MDR-3 monochromator, (*10*) FEU-18A photomultiplier, and (*11*) recorder.

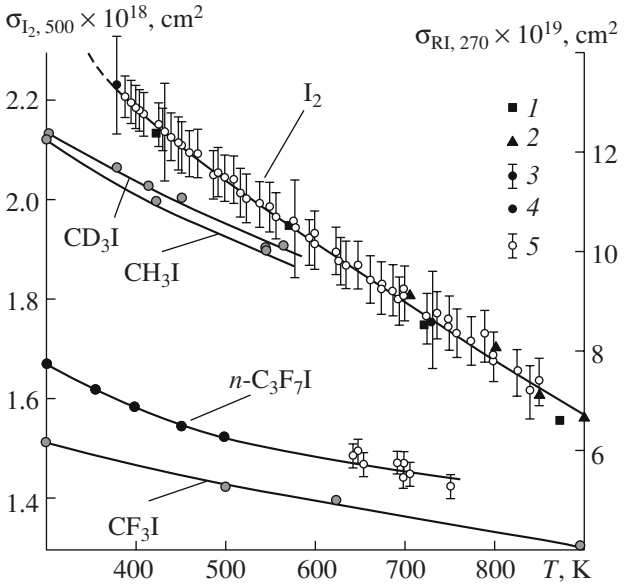

Fig. 2. Photon absorption cross section (σ) data quoted from [9–12] and measured in this work. Left-hand scale: I_2 (λ = 500 nm). Right-hand scale: CH_3I (λ = 258 nm), CD_3I (λ = 257 nm), CF_3I (λ = 267.8 nm), and n-C_3F_7I (λ = 270 nm). Sources of data: (*1*) [11], (*2*) [12], (*3*) [10], (*4*) [9], and (*5*) our measurements.

mechanism is not limited to reactions (II)–(V) either. By contrast, for the pyrolysis of the perfluorinated alkyl iodides, the overall scheme (I) and mechanism (II)–(V) are quite valid. Therefore, all alkyl iodides and bromides can be divided into the following three groups:

Group 1: Perfluoroalkyl iodides and bromides. For these compounds, the overall scheme (I) is valid and the IIP method allows the rate constant k_5 to be measured.

Group 2: The other alkyl halides except the iodomethanes. For these compounds, scheme (I) is invalid and no kinetic measurements can be made by the IIP method.

Group 3: Iodomethanes. For these compounds, the overall scheme (I) is invalid, but the ultimate product mixture is so simple that it seems possible to elucidate the pyrolysis mechanism.

In this study, we examined CF_3I, the simplest compound of group 1, in order to elucidate the role of the diffusion of the reactive species $CF_3^{\bullet}$ toward the reactor wall and to see whether it is possible to measure the rate constant k_5 as a function of the pressure of the gas being pyrolyzed (CF_3I).

The experimental setup used in our IIP kinetic studies is schematized in Fig. 1. Atmospheric oxygen was removed from the iodides and bromides by triple distillation in vacuo; water, by 24-h-long drying over zeolite (4–5) Å degassed in vacuo at T = 673 K. The reactor (Fig. 1) was filled with CF_3I using a standardized manometer (OM-2) and a vacuum system allowing the gas pressure to be reduced to 10^{-2}–10^{-4} Torr. Next, the reactor was sealed off from the system and was placed into a temperature-controlled furnace (Fig. 1). During pyrolysis, the furnace temperature was maintained with an accuracy of ±1 K. The longitudinal temperature gradient over a length of 250 mm was no higher than 1 K.

For deriving the component concentrations in the reactor from the current absorbance of the mixture being pyrolyzed (using the Bouguer–Lambert–Beer law), it is necessary to know the temperature-dependent extinction coefficients of the components. Some of these data were taken from the literature [9–12], and some were obtained by us. In some experiments, after pyrolysis the cell was cooled with liquid nitrogen and unsealed and the I_2 content of the product was determined by titration with thiosulfate. This allowed us to check, with an accuracy of ±3%, the gaseous iodine extinction coefficients (σ_{500, I_2}) reported in the literature. The extinction coefficient of the iodide was derived from its absorbance at the required wavelength and its concentration premeasured with the OM-2 manometer. The extinction coefficient data used in this study are plotted in Fig. 2.

The optical system of the kinetic setup allowed the absorbance of the reaction mixture to be measured alternately (with ±1-nm resolution and ±0.3% accuracy) at the absorption wavelength of the disappearing iodide and at the absorption wavelength of the appearing molecular iodine (Fig. 3). From the ratio of the light intensity that has passed through the cell at a given wavelength λ and cell length l (φ_l) to the intensity of the light incident on the cell end (φ_0), we derived the concentration of molecular iodine:

$$[I_2] = \frac{1}{l\sigma_{500, I_2}} \ln \frac{\varphi_0}{\varphi_l}.$$

Usually, kinetic measurements at a higher temperature were made with the same cell and for the same mixture as the lower temperature measurements. The

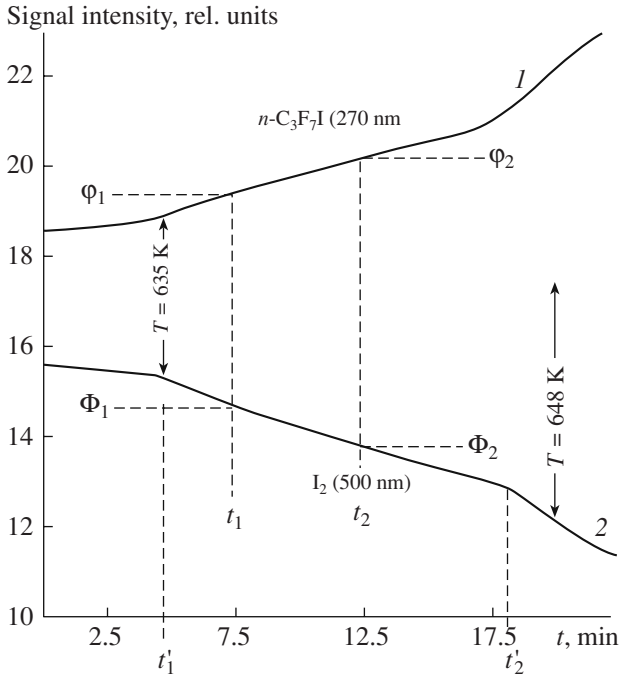

Fig. 3. Example of optical signal recording (portion of the chart of the two-channel recorder): (*1*) increasing transparence at λ = 270 nm (*n*-C_3F_7I consumption) and (*2*) decreasing transparence at λ = 500 nm (I_2 buildup). t'_1 and t'_2 are the points in time at which the temperature was raised sharply. At the point in time t_1: [RI] = 4.8×10^{17} cm^{-3}, $[I_2] = 1.45 \times 10^{16}$ cm^{-3}, and $d[I_2]/dt = 8 \times 10^{12}$ cm^{-3} s^{-1}.

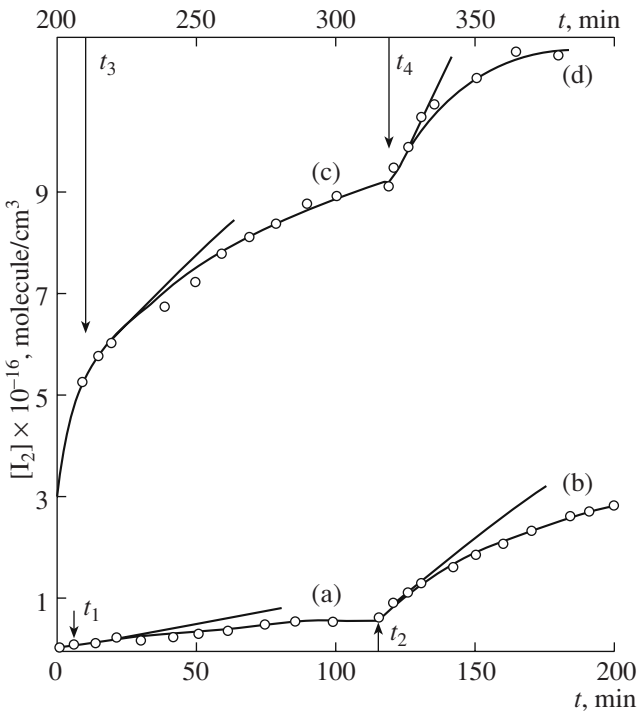

Fig. 4. I_2 accumulation kinetics in the isochoric isothermal pyrolysis of trifluoroiodomethane ($[CF_3I]_0 = 9.6 \times 10^{17}$ molecule/cm^3): (a) T_1 = 630 K for $t_1 \le t < t_2$, $\alpha = (2.0 \pm 0.7) \times 10^{-9}$ s^{-1}; (b) T_2 = 670 K for $t_2 \le t < t_3$, $\alpha = (4.8 \pm 0.5) \times 10^{-8}$ s^{-1}; (c) T_3 = 700 K for $t_3 \le t < t_4$, $\alpha = (7.4 \pm 2.0) \times 10^{-7}$ s^{-1}; (d) T_4 = 730 K for $t_4 \le t$, $\alpha = (3.2 \pm 0.3) \times 10^{-6}$ s^{-1}.

data obtained for CF_3I by such a series of measurements are shown in Fig. 4.

The data presented in Fig. 4, as well as the data obtained in other experiments, were processed using formulas (12)–(15) (see Table 2). Table 2 also lists the lifetimes of the radical $CF_3^{\bullet}$ for the recombination reaction,

$$t_{1/2} = (k_{(CF_3)_2}[CF_3])^{-1}, \quad (16)$$

Table 2. $CF_3^{\bullet}$ recombination rate constants derived from experimental data

j	$[CF_3I]_0$, Torr	T_i, K	logI_2 [cm^{-3}]	–log α [s^{-1}]	log$K_{c,2}$ [cm^{-3}]	log$K_{c,4}$ [cm^{-3}]	β_j, s^{-1}	logk_5 [cm^3/s]	$t_{1/2}$, s	
								from (15)	from (16)	from (17)
1	29.2	630	15.30 ± 0.05	8.70 ± 0.10	7.254	11.993	0.062	–11.22 ± 0.13	0.56	1.1
2		670	16.3	7.30	8.363	12.716	0.086	–11.30	0.28	1.0
3		700	16.85	6.13	9.111	13.204	0.206	–11.15	0.12	1.0
4		730	16.95	5.50	9.740	13.652	0.304	–11.32	0.08	0.9
5	298	628	16.30 ± 0.05	8.43 ± 0.07	7.195	11.954	4.3	–10.87 ± 0.07	0.06	11
6		673	17.3	6.75	8.441	12.767	9.1	–10.87	0.03	10
7		712	17.9	5.46	9.393	13.387	19.6	–10.86	0.012	10
8		732	18.0	4.85	9.841	13.680	35.0	–10.85	0.007	9

and for the diffusion loss on the wall,

$$t_{1/2} = 1/k_D. \quad (17)$$

It is clear from the data presented in the last two columns of Table 2 that, at P = 29 Torr, the contribution from $CF_3^\bullet$ diffusion from the bulk decreases rapidly from 30 to 10% as the temperature is raised from 630 to 730 K. At P = 298 Torr and all temperatures examined, the rate of the diffusion loss of the radicals is as low as thousandths of the rate of recombination (reaction (V)).

RESULTS AND DISCUSSION

For more correct data processing, we introduced a trial k_a value and solved, for the three unknowns x, y, and k_D^*, the overdetermined system of eight algebraic equations (14) corresponding to eight experimental situations (Table 2). The optimum results were obtained with the trial value

$$k_a = k_{5,\infty} = (11.0 \pm 0.5) \times 10^{-12} \sqrt{T/300\ \text{K}}\ \frac{\text{cm}^3}{\text{molecule s}} \quad (18)$$
$$(T = 300\text{–}1300\ \text{K}),$$

which is in agreement with the most reliable data from the literature (Fig. 5).

At a preset trial value of k_a, one of the equations (14) (e.g., for j = 1 in Table 2) was subtracted from the seven other equations. This reduced the system to seven equations for two unknowns, namely, x and $y = b$. Solving this overdetermined system, we obtained

$$x = 10^{0.4 \pm 0.3}, \quad y = b = (2000 \pm 500)\ \text{K}. \quad (19)$$

If we set $k^* = 3.5k_a$ from model considerations, then it will be possible to "split" x into the following two rate constants:

$$k^* = 4 \times 10^{-11} \sqrt{T/300\ \text{K}}\ \frac{\text{cm}^3}{\text{molecule s}},$$
$$k_{-a} = 10^{9.4 \pm 0.3} \exp[-(2000 \pm 500\ \text{K})/T]\ \text{s}^{-1}. \quad (20)$$

Here the preexponential factor in the expression for k_{-a} has a realistic value. Therefore, at any pressure (concentration) of the buffer gas CF_3I and any temperature in the 300–1300 K range, the sought $CF_3^\bullet$ recombination rate constant k_5 can be represented as

$$k_{(CF_3)_2}^{CF_3I} = \frac{(1.10 \pm 0.05) \times 10^{-11} \sqrt{T/300\ \text{K}}}{1 + \dfrac{10^{9.4 \pm 0.3} \exp(-(2000 \pm 500\ \text{K})/T)}{4 \times 10^{-11} \sqrt{T/300\ \text{K}}\,[CF_3I]}}\ \frac{\text{cm}^3}{\text{molecule s}}, \quad (21)$$

where the concentration $[CF_3I]$ is expressed in units of molecule/cm^3.

For k_D^*, we obtained an upper limit of 0.062 s^{-1}, to which the following diffusion coefficient corresponds:

$$D^*_{CF_3,\,CF_3I} = \frac{k_D^*}{2.6} \le 0.023\ \text{cm}^2/\text{s}. \quad (22)$$

The standard estimate is $D^*_{CF_3,\,CF_3I} = \frac{1}{3}\langle l \rangle \langle \upsilon \rangle$ = 0.01 cm^2/s [8]; that is, in the j = 1 experiment (Table 2),

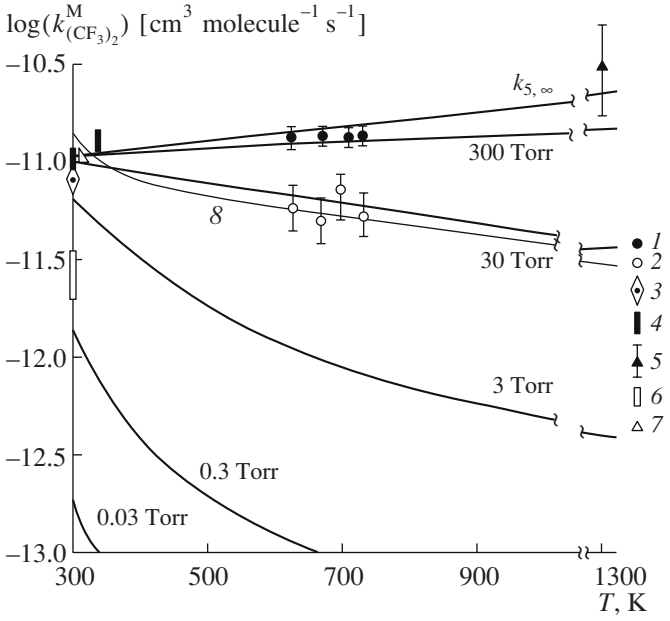

Fig. 5. Rate constant data (k_5) for $CF_3^\bullet$ recombination (reaction (V)) in the buffer gas M = CF_3I measured in this study and quoted from the literature: (*1*) k_5 for $[CF_3I]_0$ = 298 Torr, (*2*) k_5 for $[CF_3I]_0$ = 29.2 Torr, (*3*) data from [13], (*4*) data from [14], (*5*) data from [15], (*6*) data from [16], and (*7*) data from [17]. The curves are the plots of function (21) for different buffer gas pressures; (*8*) data theoretically calculated for the flexible transition state model in the high-pressure limit [18].

the $CF_3^{\bullet}$ diffusion loss rate is only 2 times lower than the recombination loss rate. The contribution from diffusion into the $CF_3^{\bullet}$ loss rate decreases rapidly as the gas temperature and pressure are increased. In the $j = 8$ experiment, it does not exceed 0.1%.

Passing to the low-pressure limit in Eq. (21) leads to a third-order rate constant (at $T = 300$–1300 K for the CF_3I buffer gas):

$$k_5^{CF_3I} = \frac{k_a k^*}{k_{-a}} = 10^{-30.8\pm0.3}\left(\frac{T}{300\ \mathrm{K}}\right)e^{\frac{(2000\pm500)\ \mathrm{K}}{T}}\frac{\mathrm{cm}^6}{\mathrm{molecule}^2\ \mathrm{s}} = 10^{-27.9\pm0.5}\left(\frac{T}{300\ \mathrm{K}}\right)^{-2.8}\frac{\mathrm{cm}^6}{\mathrm{molecule}^2\ \mathrm{s}}. \quad (23)$$

From Eq. (21), one can also derive the "half-pressure," that is, the pressure at which $k_{(CF_3)_2}^{CF_3I} = \frac{1}{2}k_{(CF_3)_2}^{\infty}$:

$$[CF_3I]_{1/2} = \frac{10^{19.8\pm0.3}}{\sqrt{T/300\ \mathrm{K}}}e^{-\frac{(2000\pm500)\ \mathrm{K}}{T}}\frac{\mathrm{molecule}}{\mathrm{cm}^3}. \quad (24)$$

For example, $[CF_3I]_{1/2} = 2.4$ Torr at 300 K, 48.2 Torr at 600 K, and 121 Torr at 900 K.

The $CF_3^{\bullet}$ recombination rate constant (21) at various temperatures and buffer gas (M = CF_3I) pressures is plotted in Fig. 5. It is clear from the totality of these data that the value of $k_{(CF_3)_2}^{\infty} = 3.9\times10^{-11}$ cm^3 molecule^{-1} s^{-1} [19], which was widely accepted earlier and was included in many respectable handbooks (see, e.g., [20]), is actually 3 times higher than the true value. Conversely, the more recent value of $k_{(CF_3)_2}^{\infty}$ (300 K) $= (5\pm1)\times10^{-12}$ cm^3 molecule^{-1} s^{-1} [16, 21, 22] is two times lower than the true value. It would be appropriate to correct the reference data for the rather numerous rate constants that were calculated using the old $k_{(CF_3)_2}^{\infty}$ value as the reference point.

It is evident from Fig. 5 that theoretical calculations in the framework of the canonical flexible transition state model [18] do not afford the correct topology of $k_{(CF_3)_2}^{\infty}$ as a function of temperature in the high-pressure limit. So, the barrierless recombination of two free radicals with the attractive dispersion potential –const r^{-6} [23] remains the best model, which implies the relationship $k_{(CF_3)_2}^{\infty} \approx T^{1/6}$.

Consider the dissociation–recombination process

$$C_2F_6 \underset{k_{rec}}{\overset{k_{dis}}{\rightleftarrows}} 2CF_3 - 397.32\ \frac{\mathrm{kJ}}{\mathrm{mol}}. \quad (\mathrm{VII})$$

Using the thermodynamic function data bank available from [24], it is possible to calculate the equilibrium constant $K_c = k_{dis}/k_{rec}$:

$$K_c = 10^{29.184}\left(\frac{T}{300\ \mathrm{K}}\right)^{-0.55}\exp\left(-\frac{47786\ \mathrm{K}}{T}\right)\frac{\mathrm{molecule}}{\mathrm{cm}^3} \quad (25)$$

in the temperature range 300–600 K,

$$K_c = 10^{29.184}\left(\frac{T}{300\ \mathrm{K}}\right)^{-1.162}\exp\left(-\frac{47786\ \mathrm{K}}{T}\right)\frac{\mathrm{molecule}}{\mathrm{cm}^3} \quad (26)$$

in the temperature range 300–1500 K.

From Eqs. (26) and (21), we can derive the rate constant of dissociation (VII) over the temperature range 300–1500 K at any pressure of the buffer gas CF_3I:

$$k_{dis}^{CF_3I} = \frac{10^{18.22\pm0.02}\left(\frac{T}{300\ \mathrm{K}}\right)^{-0.662}\exp\left(-\frac{47786\ \mathrm{K}}{T}\right)}{1 + k_{-a}/k^*[CF_3I]}\ \mathrm{s}^{-1}, \quad (27)$$

where k^* and k_{-a} are defined by Eq. (20). In the high-pressure limit, Eq. (27) reduces to

$$k_{dis}^{\infty} = 10^{18.22\pm0.02}\left(\frac{T}{300\ \mathrm{K}}\right)^{-0.662}\exp\left(-\frac{47786\ \mathrm{K}}{T}\right)\mathrm{s}^{-1}. \quad (27')$$

The rate constant of dissociation (VII) in the high-pressure limit was measured directly using a shock tube [25]:

$$k_{dis}^{\infty} = 4.3\times10^{17}\exp\left(-\frac{(47500\pm2000)\ \mathrm{K}}{T}\right)\mathrm{s}^{-1} \quad (28)$$

in the temperature range (1300–1600) K.

In particular, for the middle point of the temperature range specified in Eq. (28) (1450 K), Eq. (28) yields $k_{dis}^{\infty} = 10^{3.43\pm0.60}$ s^{-1}. This value coincides with the value following from Eq. (27') (k_{dis}^{∞} (1450 K) $= 10^{3.47\pm0.02}$ s^{-1}) within the limits of the error.

The rate constant $k_{(CF_3)_2}^{\infty}$ was measured earlier by the flash photolysis method [26, 27]. However, in order to obtain an absolutely independent result, we did not use the flash photolysis data [26, 27] when constructing the plot shown in Fig. 5. Considering the theoretical model suggested by Kondrat'ev et al. [23] and the most reliable measurements [15, 27], the following formula can be recommended instead of Eq. (21):

$$k_{(CF_3)_2}^{CF_2I} = \frac{(1.27 \pm 0.10) \times 10^{-11} (T/300\ \mathrm{K})^{0.25}}{1 + \dfrac{10^{9.4 \pm 0.3} \exp(-(2000 \pm 500\ \mathrm{K})/T)}{4 \times 10^{-11} \sqrt{T/300\ \mathrm{K}}[CF_3I]}} \frac{\mathrm{cm}^3}{\mathrm{molecule\ s}}. \quad (21')$$

For $T = 1450$ K, Eq. (21') yields $k_{dis}^{\infty} = 10^{3.35 \pm 0.04}$ s^{-1}. This value coincides with the experimental value k_{dis}^{∞} (1450 K) $= 10^{3.43 \pm 0.60}$ s^{-1} [25] within the limits of the error.

Note that the recombination of two identical radicals,

$$2R^{\bullet} + M \longrightarrow R_2 + M,$$

can be characterized either by the "small" rate constant $k_{R_2} = k_5$, as was done in our earlier study [1] and in this work (see Eq. (5)), or by the "large" rate constant

$$d[R]/dt = -k_{R_2}^{*}[R]^2, \quad (29)$$

as was done in our other works [26, 27]. Obviously, $k_{R_2}^{*} = 2k_{R_2}$. This should be remembered by Internet users because the compilers of the database available from [28] do not make any difference between k_{R_2} and $k_{R_2}^{*}$. Therefore, to avoid confusion, Internet users should always refer to the original work. For example, according to [28], our data [27] lead to a value of 2.55×10^{-11} cm^3 molecule^{-1} s^{-1} for the rate constant of recombination (VII) at 300 K. However, we used the "large" rate constant (29) in [27], so, in the notation used in this paper, $k_{(CF_3)_2}^{\infty}$ (300 K) $= \frac{1}{2}k_{R_2}^{*} = 1.27 \times 10^{-11}$ cm^3 molecule^{-1} s^{-1}. This value is in agreement with Eq. (18) and is used in Eq. (21').

REFERENCES

1. Skorobogatov, G.A., Dymov, B.P., Lebedev, V.N., and Khripun, V.K., *Kinet. Katal.*, 1987, vol. 28, no. 4, p. 785.
2. Tedeev, R.Sh., Dymov, B.P., and Skorobogatov, G.A., *Vestn. Leningr. Univ., Ser. 4: Fiz. Khim.*, 1989, no. 4, p. 37.
3. Skorobogatov, G.A., Dymov, B.P., and Tedeev, R.Sh., *Zh. Obshch. Khim.*, 1991, vol. 61, no. 1, p. 178.
4. Skorobogatov, G.A., Dymov, B.P., and Khripun, V.K., *Kinet. Katal.*, 1991, vol. 32, no. 2, p. 252.
5. Troe, J., *Ann. Rev. Phys. Chem.*, 1978, vol. 29, p. 223.
6. Kondrat'ev, V.N., *Kinet. Katal.*, 1967, vol. 8, no. 5, p. 965.
7. Semenov, N.N., *O nekotorykh problemakh khimicheskoi kinetiki i reaktsionnoi sposobnosti* (On Some Problems of Chemical Kinetics and Reactivity), Moscow: Akad. Nauk SSSR, 1958.
8. Zubarev, D.N., in *Fizicheskaya entsiklopediya* (Encyclopedia of Physics), Moscow: Sovetskaya Entsiklopediya, 1988, vol. 1, p. 686.
9. Elokhin, V.A. and Ivanov, V.S., *Zh. Prikl. Spectrosk.*, 1980, vol. 33, no. 4, p. 759.
10. Broadbent, T.W. and Callear, A.B., *Trans. Faraday Soc.*, 1971, vol. 67, no. 10, p. 3030.
11. Sulzer, P. and Wieland, K., *Helv. Phys. Acta*, 1962, vol. 25, p. 653.
12. Tellinghuisen, J., *J. Chem. Phys.*, 1973, vol. 58, p. 2821.
13. Hiatt, R. and Benson, S., *Int. J. Chem. Kinet.*, 1972, vol. 4, no. 5, p. 479.
14. Ogawa, T., Carlson, G.A., and Pimentel, G.C., *J. Phys. Chem.*, 1970, vol. 74, p. 2090.
15. Glanzer, K., Maier, M., and Troe, J., *J. Phys. Chem.*, 1980, vol. 84, no. 13, p. 1681.
16. Selamoglu, N., Rossi, M.J., and Golden, D.M., *Chem. Phys. Lett.*, 1986, vol. 124, no. 1, p. 68.
17. Pagsberg, P., Jodkowski, J.T., Ratajczak, E., and Sillesen, A., *Chem. Phys. Lett.*, 1998, vol. 286, p. 138.
18. Pesa, M., Pilling, M.J., Robertson, S.H., and Wardlaw, D.M., *J. Phys. Chem. A*, 1998, vol. 102, p. 8526.
19. Ayscough, P.B., *J. Chem. Phys.*, 1956, vol. 24, p. 944.
20. Kondrat'ev, V.N., *Konstanty skorosti gazofaznykh reaktsii* (Rate Constants of Gas-Phase Reactions), Moscow: Nauka, 1970.
21. Basco, N. and Hathorn, F.G.M., *Chem. Phys. Lett.*, 1971, vol. 8, p. 291.
22. Ershov, L.S., Zalesskii, V.Yu., and Sokolov, V.N., *Kvantovaya Elektron.*, 1978, vol. 5, no. 4, p. 863.
23. Kondrat'ev, V.N., Nikitin, E.E., Reznikov, A.I., and Umanskii, S.Ya., *Termicheskie bimolekulyarnye reaktsii v gazakh* (Thermal Bimolecular Reactions in Gases), Moscow: Nauka, 1976.
24. Gurvitch, L.V., Khachkuruzov, G.A., Medvedev, V.A., et al., *Termodinamicheskie svoistva individual'nykh veshchestv* (Thermodynamic Properties of Individual Substances), Glushko, V.P., Ed., Moscow: Nauka, 1978.
25. Tschuikow-Roux, E., *J. Chem. Phys.*, 1965, vol. 43, no. 7, p. 2251.
26. Skorobogatov, G.A., Seleznev, V.G., and Slesar, O.N., *Dokl. Akad. Nauk SSSR*, 1976, vol. 231, no. 6, p. 1407.
27. Skorobogatov, G.A., Slesar', O.N., and Torbin, N.D., *Vestn. Leningr. Univ., Ser. 4: Fiz. Khim.*, 1988, no. 4, p. 30.
28. http://kinetics.nist.gov/kinetics/.